

# Tropical Cyclone Wind Waves in the Gulf of Mexico under a Changing Climate

Christian M. Appendini<sup>1</sup>, Pablo Ruiz-Salcines<sup>1</sup>, Rodrigo Duran<sup>2,3</sup>

<sup>1</sup> Laboratorio de Ingeniería y Procesos Costeros, Instituto de Ingeniería, Universidad Nacional Autónoma de México, Puerto de abrigo s/n, Sisal, Yucatán 97356, México.

<sup>2</sup> National Energy Technology Laboratory, 1450 Queen Avenue SW, Albany, OR

<sup>3</sup> Theiss Research, La Jolla, CA, 92037, USA

Corresponding author: Christian M. Appendini ([cappendinia@iingen.unam.mx](mailto:cappendinia@iingen.unam.mx)), ORCID: 0000-0002-6044-3351

## Key Points:

- The use of physics-based synthetic tropical cyclones allows projections of extreme wave climate in tropical cyclone-prone regions
- Extreme ocean waves are expected to increase between 5-20% (north) and 15-35% (south) in the Gulf of Mexico by the end of the century
- As the climate warms, the use of non-stationary wave climates for design reduces failure probability

## **Abstract**

The expected rise in major tropical cyclones due to climate change will increase their associated hazards, including ocean waves which are the main design parameter for maritime structures. To assess how climate change will affect tropical cyclone waves in the Gulf of Mexico we use physics-based synthetic tropical cyclones derived for present and future climates, overcoming the limitations imposed by insufficiently long records and inadequate resolution in General Circulation Models. Using events derived from six Coupled Model Intercomparison Project Phase 5 models, we estimate the probability of extreme waves for the present climate, and global warming under the Representative Concentration Pathway 8.5 scenario. The results show the importance of non-stationary wave climates for planning and design of maritime structures to reduce structure failure probability as we transit into a future climate with an increased probability of extreme waves.

## **Plain Language Summary**

Climate change studies on tropical cyclones predict that the most intense events will be more likely by the end of the century, increasing exposure to their hazards. Ocean waves from tropical cyclones are a destructive force acting directly on maritime structures and are one of the main design parameters for structures. As such, the question of how climate change will affect the extreme waves by the end of the century is paramount for adequate planning. We use physics-based synthetic tropical cyclones to overcome inadequate data and study wind waves in the Gulf of Mexico under present and future climates, finding that extremes waves will be larger by the end of this century. The design of maritime structures should account for a changing climate to correctly estimate the probability of damage and failure during their lifetime.

## **1 Introduction**

Tropical cyclone (TC) derived wind waves determine structural design conditions for maritime structures in TC prone regions, such as in the Gulf of Mexico (GoM) where offshore oil and gas extraction activities started in 1937 (Horowitz, 2020), with continuous extraction since 1948 (Dunn, 1994). Despite the importance of waves, no guidance for design wave parameters was issued for designing structures during the first decades of oil and gas activities (Dunn, 1994; Wisch et al., 2004). Hurricanes Hilda (1964) and Betsy (1965) forced the industry

to recognize the importance of understanding extreme events so that the American Petroleum Institute (API) created its Offshore Committee, and in 1969 the API released its first standard (Wisch et al., 2004). However, design wave recommendations appeared until the 7th edition of RP 2A in 1976, where the 100-year return period was recommended as the design wave (Mangiavacchi et al., 2005). Since then, a series of hurricanes have struck the GoM oil and gas extraction areas, generating severe damages and operational down-time (Austin et al., 2008; Cruz & Krausmann, 2008; Kaiser & Yu, 2010), leading the API to update the recommended wave design parameters. After hurricane Ivan (2004) and the highly active 2005 hurricane season, the API release updated design recommendations by dividing the GoM into different regions and providing wave design parameters for each of them (API, 2007). Acknowledging the intensity of hurricanes Ivan (2004), Katrina (2005), Rita (2005), and Ike (2008), and that a particular intense hurricane or hurricane season can modify the extreme wave statistics (Panchang et al., 2013), API recommendations were updated again in 2014 (API, 2014). API recommendations are based on historical data (Supplementary Information Text S1), so updates are required as new extreme events are incorporated. The fact that wave statistics change by incorporating recent extreme events is evidence that the observation record is too short to provide robust statistics and/or that climate change is affecting extreme waves. In either case, the need for constant update of design recommendations based on historical events leads to uncertainties on structures stability.

Considering the short historical record hindering a robust wave climate characterization, and that climate change is expected to modify the future climate where the most extreme TCs (i.e. categories 4 and 5 in the Saffir-Simpson scale) are expected to increase in proportion by the end of the century (Knutson et al., 2020), synthetic TCs can be used to obtain robust statistics for the present climate and to generate wave climate projections towards the end of the century. Synthetic events are events derived from simplified models, created specifically to generate physics-based tropical cyclones and not the events found in atmospheric-ocean models (e.g. Global Circulation Models) in which tropical cyclones are generated according to the processes resolved by the models. The limitation and advantages of using TCs directly or dynamically downscaled from Global Circulation Models (GCMs) versus synthetic TCs, to characterize future TC climates, are highlighted in Emanuel (2021); the main disadvantage for synthetic events is the lack of feedback between the large-scale environment and the downscaled events

which may lead to an overestimation of events. Considering the advantages of synthetic events, Appendini et al. (2017) presented an assessment of the extreme wave climate in the GoM considering global warming using synthetic TCs derived from RCP 4.5 and 8.5 scenarios and two different GCMs, finding that the 100-year design wave can be up to 5 m higher when considering global warming instead of the present climate. This study showed the relevance of including climate change into the design parameters, as the coastal and offshore structures that we design this decade, will be operating during future climate conditions. Still, there is large uncertainty in their study as it only considers two GCMs.

Efforts done by the scientific community under the COWCLIP framework (Hemer et al., 2012), have already produced wave projection ensembles to identify robust changes in the wave climate by the end of the century (Morim et al., 2019). Nevertheless, the challenges to resolve extreme waves in TC-affected areas have been acknowledged, due to the low GCMs resolution used to force the wave models (Morim et al., 2019), affecting storm size, intensity, structure, and translational speed (Timmermans et al., 2017), and the small number of TCs in the GCMs (Mori et al., 2010). Both issues have been reported in studies related to TC projections in a future climate (Camargo, 2013; Emanuel, 2010; Hill & Lackmann, 2011; Knutson et al., 2020). While recent studies analyzing TCs from storm resolving models (Judt et al., 2021) and CMIP6 HighResMIP (Roberts et al., 2020a; Roberts et al., 2020b) show improvements in the representation of TCs, the use of synthetic TCs pose an alternative to overcome the underestimation of TCs and their wind speeds in GCMs. The use of synthetic events allows robust characterization of extreme events by overcoming the short observational record, and it also allows sampling extreme-wave conditions under projected future climate in TC-prone areas. This work aims to provide an alternative method to determine extreme wave conditions in the GoM following Appendini et al. (2017), aiming to highlight the importance of using non-stationary wave climates for planning and design of offshore structures.

## **2 Materials and Methods**

To assess the extreme wave climate in the GoM we followed the methodology used by Appendini et al. (2017), as summarized in Figure S1. The extreme wave climate was obtained by using synthetic TCs derived from reanalysis and GCMs as described in section 2.1, from which

we created wind fields using a parametric wind model to force a third-generation wave model. The following subsections summarize each of the methodological steps.

## 2.1 Synthetic tropical cyclones database

The synthetic events datasets were derived following Emanuel et al. (2006, 2008) and Emanuel (2013). As summarized by Appendini et al. (2017), the generation of the synthetic events consists of the random seeding of warm-core vortices across the ocean with peak wind speeds of 12 m/s that can either develop (by reaching an intensity of at least 21 m/s) or decay according to the large-scale oceanic and atmospheric conditions. The events are stirred by a beta-advection model (Marks, 1992), and the intensity of the events is calculated along each track position using the model by Emanuel (2004). Both models use synthetic wind time series at 250 and 850 hPa, represented as Fourier series of random phase, constrained to have the monthly means, variances, and covariances calculated using daily data from reanalyses or GCM, and to have a geostrophic turbulence power-law distribution of kinetic energy (Emanuel et al., 2008). Hence, tracks and forward velocities are determined by the ambient circulation. The intensity model also considers the monthly mean potential intensity and 600 hPa temperature and specific humidity derived from the reanalysis or GCM (Emanuel, 2013).

The synthetic TCs databases for the present and future climates encompass the events derived using six different GCM from the Coupled Model Intercomparison Project Phase 5 (CMIP5): GFDL, HADGEM, IPSL, MIROC, MPI, and CCSM (refer to table S1 for the complete name of each model, version, and reference). For a future climate, we used Representative Concentration Pathway 8.5 (RCP 8.5) scenario (Moss et al., 2010). The present climate is considered for the years from 1975 through 2005 and a future climate from 2070 through 2100 (except for HADGEM which goes from 2069 through 2099). The synthetic events on each database consist of 3000 events for the reanalysis and GCM derived events for the North-Atlantic basin. However, we followed Appendini et al. (2017) and only used the synthetic TCs entering the GoM and the western Caribbean Sea, which encompass the numerical domain of the wave model. The number of events entering the wave model domain is a reduced subset of each database (Table S2) and were used to force the wave model. The validation of the synthetic database is presented in Appendini et al. (2019), where the NCEP/NCAR (NCEP) wind

reanalysis (Kalnay et al., 1996) derived events were validated using the Hurricane Database (HURDAT2) dataset (Landsea & Franklin, 2013).

## 2.2 Wave modeling

To obtain the wave conditions for each of the TC in the synthetic databases, we first obtained the wind fields for each event, as described in Text S2. The resulting wind fields, with a resolution of  $0.11^\circ$ , were used to force the MIKE 21 SW wave model (Sørensen et al., 2004), which is a flexible mesh, finite volume model based on the wave action equation to simulate the growth, decay, and transformation of wind-generated waves. The wave model domain encompassed the GoM and the western Caribbean Sea, with boundaries along the  $80^\circ\text{W}$  longitude and  $15^\circ\text{N}$  latitude. A computational mesh based on triangular elements of approximately 10 km was created using ETOPO1 bathymetric data (Amante & Eakins, 2009) and available local surveys for the Mexican coastal areas. For details on the wave model, setup and validation please refer to Appendini et al. (2017). Here we used 32 bins for the directional discretization instead of 17 to mitigate the garden sprinkler effect (Tolman, 2002) over the wave period. While Appendini et al. (2017) mentioned that the garden sprinkler effect is mitigated when analyzing the maximum value maps for significant wave height (SWH), it is not the case for wave period, thus we decided to increase the directional spectral resolution. We validated the wave model by simulating historical events from 1975 to 2020 and comparing the model results to NDBC buoys as represented by their inverse cumulative distributions (Text S3 and Figure S2). The resulting statistics are shown in Table S3. Correlation analysis resulted in correlation coefficient values larger than 0.95 for  $H_s$ .

## 2.3 Wave analysis

For each synthetic event, we calculated the wave fields such as SWH, peak wave period (PWP), and mean wave direction (MWD), thus having the same number of maps for each variable as the number of synthetic events (Table S2). Using the individual maps of maximum values, we characterized the extreme wave climate by taking mean values or specific percentiles. In this article, we are only presenting the results related to SWH. Furthermore, we characterize the extreme wave probability using the return period, which is commonly used to define the design wave criteria. As such, we characterized the SWH for different return periods both for

each mesh element in the wave model and for the API (2014) regions defined for the northern GoM, as described in Text S4.

### 3 Results and discussion

#### 3.1. Bias assessment for waves derived from GCM derived synthetic events

The validated wave model was forced with NCEP and GCM derived synthetic events to characterize the wave climate from each dataset. Considering the short historical record, the NCEP derived wave climate was used as a baseline to assess the bias of the present wave climate from GCM-derived events. We use this approach because the NCEP/NCAR simulation is our best approximation of ambient conditions for the seeding of synthetic events, as it is a reanalysis based on observations. For each synthetic event, we created a map with the resulting maximum SWH field, and using all the maxima fields from each simulated event, we computed the mean, 90%, 95%, and 99%-iles for each database. The present-day wave climate bias was obtained for each of the six GCM derived events using the NCEP derived wave climate. For a clearer discussion, the model domain is divided into four sectors referred to as northwestern (NW), northeastern (NE), southwestern (SW), and southeastern (SE) regions. Figure 1 shows the bias for the model ensemble, where a general underestimation of the mean SWH is found in the entire study area and higher biases in the NW and SE regions (Figure 1a). The same occurs for the 99%-ile model ensemble, where the bias is reduced, with some overestimations offshore Louisiana, Mississippi, western and southern Florida, and the northwestern Yucatan Peninsula (Figure 1b).

As a reference, Figure S3 shows the mean, 90%, 95%, and 99%-iles for the NCEP derived events. The NW events affect the offshore areas of Texas, Louisiana, and northern Mexico, the NE affects offshore areas West Florida and Mississippi, as well as the north part of the loop current, the SW the Campeche sound and the SE the western Caribbean Sea, the Yucatan current and the southern part of the loop current. The results show that the highest events are found in the northern section of the GoM (NW and NE) as well as in the northern part of the SE region, while the SW region is the area with the milder TC-derived waves. For the individual GCMs, Figure S4 shows the bias when considering the mean values and Figure S5 when considering the 99%-ile. The bias considering mean values (Figure S4) shows high

variability between models, where some overestimate in the NE region (HADGEM, IPSL, and MIROC), others in the SW and SE GoM (GFDL and MPI), while CCSM shows a general underestimation and HADGEM a large underestimation in the SE region. Similar bias patterns are obtained for the 99%-ile (Figure S5), although the bias is less smooth and intensified, particularly in locations such as the Mexican GoM in sector SW in HADGEM or the NE sector in IPSL. Yet, the bias is reduced considerably when considering the model ensemble (Figure 1).

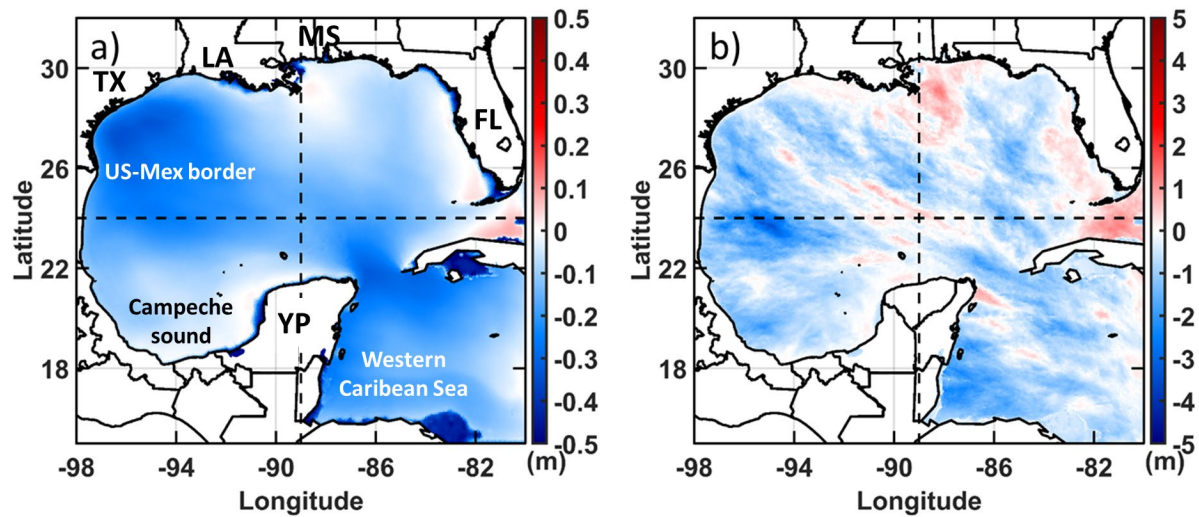


**Figure 1.** Significant wave height bias for the Global Circulation Models ensemble considering a) mean and b) 99%-ile values. Acronyms for text in a) TX=Texas, LA=Louisiana, MS=Mississippi, FL=Florida, YP=Yucatan Peninsula.

### 3.2. Future wave climate assessment

A future wave climate was obtained from the models' ensemble and compared to the present wave climate as obtained from GCM derived synthetic events. For the comparison, we used the mean values and percentiles (Figure 2). The results show a general increase for the mean waves and the percentiles, where the highest increases in wave height are in the NE followed by the SE. The relative increase (based on percentage increase) is higher in the SW for higher percentiles, corresponding to the Campeche Sound where most oil and gas activities in Mexico take place. These results are consistent with the trends reported by Ojeda et al. (2017) in the Mexican GoM. The regions in the NE and eastern NW are where SWH increases the most in a future climate, and correspond to the oil and gas areas near Louisiana. Present and future wave



conditions for each GCM are shown in Figure S6 and S7 respectively, and the projected wave  
climate for each GCM is discussed in Text S5.

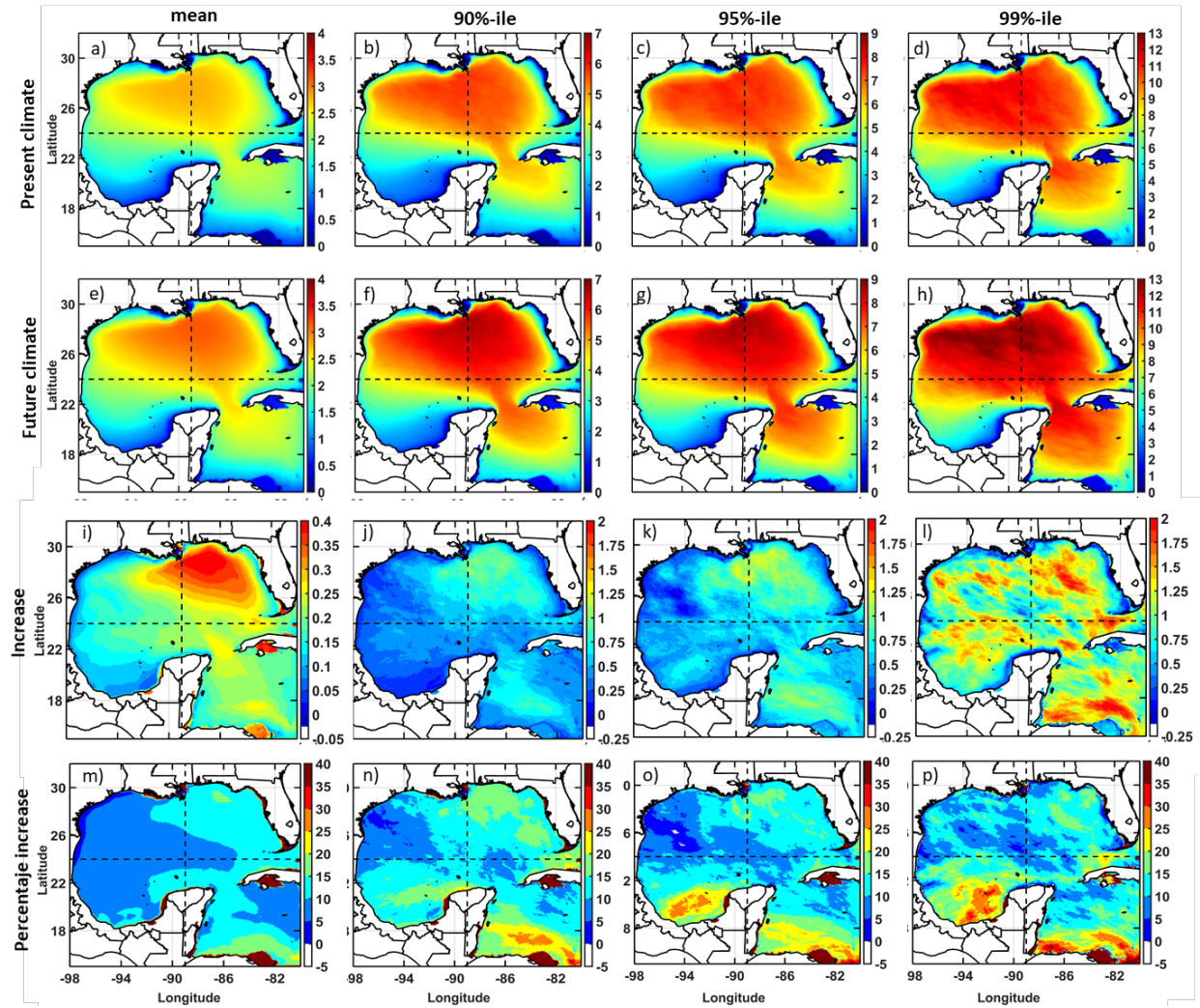


**Figure 2.** Wave conditions for significant wave height for the present (a, b, c, d) and a future (e, f, g, h) wave climate model ensembles, as well as the increase in significant wave height (i, j, k, l) and in percentage (m, n, o, p) in the future with respect to the present climate. Results show mean (a, e, i, m), 90%-ile (b, f, j, n), 95%-ile (c, g, k, o) and 99%-ile (d, h, l, p).

### 3.3. Wave conditions based on return periods and implications on design

In the previous section we divided the GoM into four regions to describe our results, however, the API recommendations report SWH for different return periods within three regions

specific to US GoM waters, as shown in Figure 3 (West, Central, and East US) and defined in Text S4. To determine the wave conditions in a particular area for different return periods, API (2014) recommends grid pooling (Heideman & Mitchell, 2009) due to the low frequency of occurrence and relatively small size of the TCs and population acknowledging the randomness on storm tracks, which could have varied if slightly different ambient conditions were dominating at a particular time of the storm. Using an ensemble of TCs waves derived from different GCMs partially solves the issue of randomness and population size as TC tracks and storm specifics vary differently and independently of one another, yet, we perform a simplified grid pool analysis for the API areas (Text S4). As the 100-year return period is commonly used as the design wave parameter (e.g. API recommendations), we use it to represent the probability of a particular wave occurring in the area. Figure 3 shows the 100-year return period wave map for the GoM ensemble under present (Figure 3a) and future (Figure 3b) conditions, showing the regions defined by API (2014) for different return periods (West, Central, and East US). The ensembles were constructed using the resulting waves from the synthetic events derived from all the GCMs. Considering the 100-year return period for design, most of the GoM will experience an increase in the SWH, except for the southern part of the SW sector. API regions will experience a significant increase in SWH, including the oil and gas exploitation areas offshore Texas and Louisiana. The individual maps for each GCM are found in figures S8 and S9 for the present and future climates respectively.

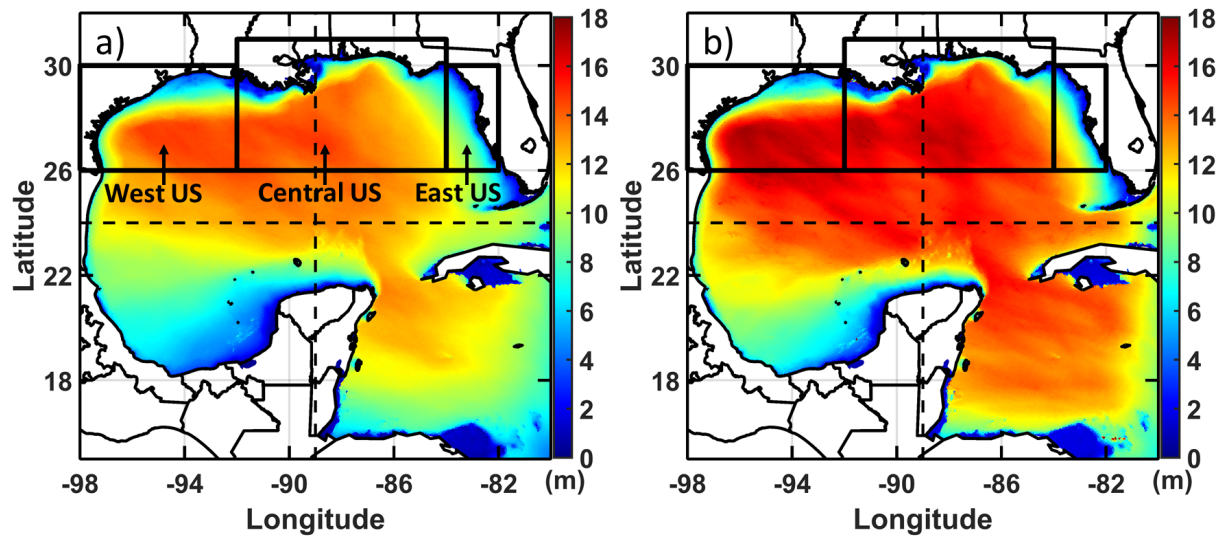


**Figure 3.** Significant wave height for the 100-year return period obtained from the GCM derived events ensemble for the (a) present and (b) future wave climates. Solid black boxes represent areas defined by API recommendations.

API (2014) does not specify the procedure to determine SWH return periods, and only refers to Oceanweather Inc., (2015) where no information is provided regarding the analysis for API regions, and thus we are unable to replicate their results. Nonetheless, we included the values reported by API (2014) for the different return periods, since they based their estimates on historical data, which is contextualized here to show the need for alternative methods to derive wave climates and account for climate change. We compared the values reported by API (2014) with those obtained using the peak over threshold method and applying the Generalized Pareto distribution to determine the return period  $H_s$  values (Text S4). Figure S10 shows that the API values are smaller than our results using synthetic events, except for the East area where API is enclosed by the uncertainty envelope of the present climate. While the underestimation by API could be a result of their method, with the use of synthetic events, higher wave height estimates are expected, as relatively short historical events will likely underestimate low probability events (i.e. the higher intensity events) even though they are plausible events and are thus represented in the synthetic events. Also, the lack of feedback between the large-scale environment and the downscaled events may lead to an overestimation of events (Emanuel, 2021). Nevertheless, the results indicate that the use of data derived from historical events can lead to underestimation of

extreme waves in a future climate. Here we note that the goal of this study is not to assess API values but to research relative changes in wave climate by the end of the century by means of synthetic events, given a changing climate according to GCM projections. As the API (2014) return-period values are the industry standard, we would like to highlight changes in future wave climate with respect to current API values. To make them directly comparable, we corrected the probability distribution of the waves derived from synthetic events based on the difference between the extreme value distribution from reanalysis-derived waves and API (2014) values. The SWHs for different return periods are shown in Figure 4. There is a good agreement between the API-Reanalysis (referred to as API hereafter) values and those from synthetic events derived from the GCMs ensemble mean for the West and Central areas, where the present climate uncertainty envelope encompasses the API values. For the East area, the API values are above the uncertainty envelope of the GCM derived events, except for return periods above 300 years. The difference between the ensemble mean and API values is about 2 m for smaller return periods, decreasing as the return period increases; both values tend to converge for West and Central areas, but not for the East. The best agreement between datasets occurs in the Central area where most oil and gas activities are located.

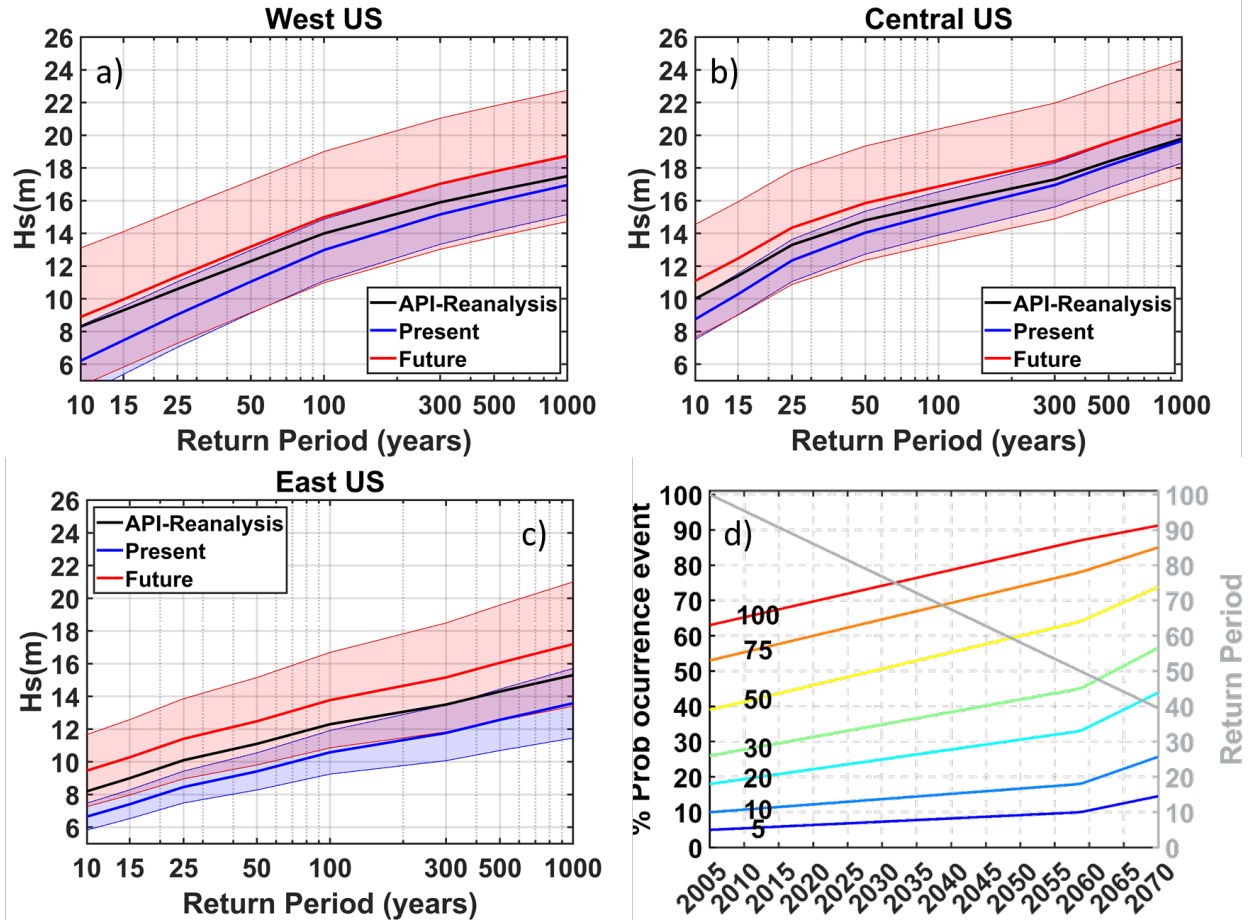


**Figure 4.** Significant wave height probability in return periods for the different API defined regions in the northern GoM (denoted with the solid black line boxes in (a) and (b) of Figure 3), a) West US, b) Central US, and c) East US, showing the return period curves for API and bias-adjusted synthetic events for the present and future climates as obtained from the GCM derived events ensemble; d) shows the percentage chance (left ordinate) of a 100-year return period wave in the present climate to occur as we transit into a future climate, where the color lines indicate the projected design life of a structure, and the gray line shows the diminishing return period value (right ordinate) of the present climate 100-year return period wave as we approach a future climate.

Present climate events (API and GCM derived events) show a lower SWH than those for a future climate (ensemble mean), while the GCM SWH ensemble mean of projected events indicate an increase between 1.3 and 3.6 m under future conditions. Please note that while there is a clear difference in the ensemble mean between present and future climate, the uncertainty envelope for the future climate encompasses the uncertainty envelope for the present climate. If we use present wave climate conditions to determine the probability of a certain wave height, we

could underestimate such probability as we approach the end of the century, as the results suggest that the extreme wave climate will be affected by the influence of global warming over TCs. Conversely, future wave climate estimates would overestimate the probability of an event early in the century. An alternative approach would be to consider non-stationary wave climates, calculating the change of probability of a certain wave height as climate change affects the extreme wave conditions deriving from TCs. This is exemplified for the Central area with Figure 4d, in which we consider the present wave climate to represent conditions in 2005 and the future wave conditions to represent conditions in 2070, while the wave conditions between 2005 and 2070 are assumed to vary linearly. In Figure 4d we used the 100-year return period in the present climate for the Central area, which equals a SWH of 13 m, corresponding to a return period of approximately 47 years in the future climate, where the gray line represents the change of return period linearly interpolated between 2005 and 2070. Each color line in Figure 4d represents a design life for a structure, showing curves for design life between 5 and 100 years, for which the left axis shows the probability of the design wave occurring during the lifetime of the structure, as derived from (CIRIA-CUR-CETMEF, 2007). For instance, a design wave of 100 years using the present climate will have a probability of occurrence of 63% in 2005 for a 100-year design life, and 26% for a 30-year design life, and the probability of occurrence as we approach 2070 will increase to approximately 91% and 57%, respectively. The high probability of occurrence in a future climate indicates that values exceeding the design waves will also increase their probability, leading to an increase in the probability of failure for structures designed using a stationary wave climate based on the present conditions.

## 5 Conclusions

We provided an assessment of the wave climate under climate change using a methodology based on synthetic TCs to overcome limitations imposed by GCMs regarding the frequency of TCs and their underestimation of maximum winds. We find that climate change in the GoM will impact TC-derived waves, increasing the probability of higher waves in the northern GoM and the western Caribbean Sea. The increase in SWH between 5-35% in a future climate and of the design waves in the order of 2 m, imply a probability of higher damage for structures that are designed considering a stationary wave climate. The probability of the design wave occurring increases towards the end of the century with climate change, and therefore a



non-stationary wave climate is needed to account for this. API standards are the oil and gas industry reference for wave design parameters, yet we show how the use of data derived from historical events can lead to the underestimation of extreme waves in a future climate. Thus, we show the need to use non-stationary wave climates to adequately account for, and reduce, the probability of structural design failure. The methodology proposed using physics-based synthetic TCs provides an alternative to determine extreme wave climates in TC-prone areas affected by climate change.

## Acknowledgments

Centro Mexicano de Innovación en Energía del Océano, CEMIE-Océano (OLE-1), UNAM-DGAPA PAPIIT Project IA100418, and the U.S. Department of Energy's Office of Fossil Energy and Carbon Management, Upstream Research Division Office of Oil and Gas (through a support contract) provided funding for this study. We want to thank Professor Kerry Emanuel for supplying the synthetic events used in this study and his advice on the analysis, as well as Gonzalo Uriel Martín-Ruiz, José López-Gonzalez, Camilo Valdéz-Rendon, and Juan Alberto Gómez-Liera for their technical assistance in this work. We also want to acknowledge Rafael Meza-Padilla and Ana Ramirez-Manguilar for their contributions in the early stages of this study. There are no real or perceived financial conflicts of interest for any author. Neither the United States Government nor any agency thereof, nor any of its employees, nor the support contractor, nor any of their employees, makes any warranty, express or implied, or assumes any legal liability or responsibility for the accuracy, completeness, or usefulness of any information, apparatus, product, or process disclosed, or represents that its use would not infringe privately owned rights. Reference herein to any specific commercial product, process, or service by trade name, trademark, manufacturer, or otherwise does not necessarily constitute or imply its endorsement, recommendation, or favoring by the United States Government or any agency thereof. The views and opinions of authors expressed herein do not necessarily state or reflect those of the United States Government or any agency thereof.

## Data availability

The data used in this study is available at

[https://figshare.com/articles/dataset/Data\\_supporting\\_Tropical\\_Cyclone\\_Wind\\_Waves\\_in\\_the](https://figshare.com/articles/dataset/Data_supporting_Tropical_Cyclone_Wind_Waves_in_the)

[Gulf of Mexico under a Changing Climate/16806877](#) with license CC BY 4.0 upon acceptance of the manuscript. The original synthetic tropical cyclone datasets used in this study are freely available from Kerry Emanuel for research purposes. For the details and availability of the synthetic datasets, please refer to Emanuel (2021) (DOI: <https://doi.org/10.1175/JCLI-D-20-0367.1>).

## References

- Amante, C., & Eakins, B. W. (2009). *ETOPO1 1 Arc-Minute Global Relief Model: Procedures, Data Sources and Analysis*.
- API. (2007). Interim Guidance on Hurricane Conditions in the Gulf of Mexico. *API Recommended Practice, 2INT-MET*, 54.
- API. (2014). Derivation of Metocean Design and Operating Conditions. ANSI/API Recommended practice 2MET. *API Recommended Practice, 2MET*(First Edition), 178.
- Appendini, C. M., Pedrozo-Acuña, A., Meza-Padilla, R., Torres-Freyermuth, A., Cerezo-Mota, R., López-González, J., & Ruiz-Salcines, P. (2017). On the Role of Climate Change on Wind Waves Generated by Tropical Cyclones in the Gulf of Mexico. *Coastal Engineering Journal*, 59(2), 1740001-1-1740001–32. <https://doi.org/10.1142/S0578563417400010>
- Appendini, C. M., Meza-Padilla, R., Abud-Russell, S., Proust, S., Barrios, R. E., & Secaira-Fajardo, F. (2019). Effect of climate change over landfalling hurricanes at the Yucatan Peninsula. *Climatic Change*, 157(3–4), 469–482. <https://doi.org/10.1007/s10584-019-02569-5>
- Austin, D. E., Priest, T., Penney, L., Pratt, J., Pulsipher, A. G., Abel, J., & Taylor, J. (2008). *History of the offshore oil and gas industry in southern Louisiana*. (Vol. Volume I:).
- Camargo, S. J. (2013). Global and regional aspects of tropical cyclone activity in the CMIP5 models. *Journal of Climate*, 26(24), 9880–9902. <https://doi.org/10.1175/JCLI-D-12-00549.1>
- CIRIA-CUR-CETMEF. (2007). *The Rock Manual. The use of rock in hydraulic engineering* (2nd editio). London: C683, CIRIA, London. Retrieved from <https://www.kennisbank-waterbouw.nl/DesignCodes/rockmanual/>



- Cruz, A. M., & Krausmann, E. (2008). Damage to offshore oil and gas facilities following hurricanes Katrina and Rita: An overview. *Journal of Loss Prevention in the Process Industries*, 21(6), 620–626. <https://doi.org/10.1016/j.jlp.2008.04.008>
- Dunn, F. P. (1994). Deepwater Production: 1950-2000. *Proceedings of the Annual Offshore Technology Conference*, 921–928. <https://doi.org/10.4043/7627-MS>
- Emanuel, K. (2004). Tropical Cyclone Energetics and Structure. *Atmospheric Turbulence and Mesoscale Meteorology*, (1944), 165–192. <https://doi.org/10.1017/cbo9780511735035.010>
- Emanuel, K. (2010). Tropical cyclone activity downscaled from NOAA-CIRES Reanalysis, 1908–1958. *Journal of Advances in Modeling Earth Systems*, 2. <https://doi.org/10.3894/james.2010.2.1>
- Emanuel, K. (2013). Downscaling CMIP5 climate models shows increased tropical cyclone activity over the 21st century. *Proceedings of the National Academy of Sciences of the United States of America*, 110(30), 12219–12224. <https://doi.org/10.1073/pnas.1301293110>
- Emanuel, K. (2021). Response of Global Tropical Cyclone Activity to Increasing CO<sub>2</sub>: Results from Downscaling CMIP6 Models. *Journal of Climate*, 34(1), 57–70. <https://doi.org/10.1175/JCLI-D-20-0367.1>
- Emanuel, K., Ravela, S., Vivant, E., & Risi, C. (2006). A statistical deterministic approach to hurricane risk assessment. *Bulletin of the American Meteorological Society*, 87(3), 299–314. <https://doi.org/10.1175/BAMS-87-3-Emanuel>
- Emanuel, K., Sundararajan, R., & Williams, J. (2008). Hurricanes and Global Warming: Results from Downscaling IPCC AR4 Simulations. *Bulletin of the American Meteorological Society*, 89(3), 347–367. <https://doi.org/10.1175/BAMS-89-3-347>
- Heideman, J. C., & Mitchell, D. A. (2009). Grid Point Pooling in Extreme Value Analysis of Hurricane Hindcast Data. *Journal of Waterway, Port, Coastal, and Ocean Engineering*, 135(2), 31–37. [https://doi.org/10.1061/\(ASCE\)0733-950X\(2009\)135:2\(31\)](https://doi.org/10.1061/(ASCE)0733-950X(2009)135:2(31))
- Hemer, M. A., Wang, X. L., Weissse, R., & Swail, V. R. (2012). Advancing wind-waves climate science: The COWCLIP project. *Bulletin of the American Meteorological Society*, 93(6), 791–796. <https://doi.org/10.1175/BAMS-D-11-00184.1>

- 422 Hill, K. A., & Lackmann, G. M. (2011). The impact of future climate change on TC intensity and  
423 structure: A downscaling approach. *Journal of Climate*, 24(17), 4644–4661.  
424 <https://doi.org/10.1175/2011JCLI3761.1>
- 425 Horowitz, A. (2020). *Katrina: A History, 1915–2015* (First). Cambridge: Harvard University  
426 Press.
- 427 Judt, F., Klocke, D., Rios-Berrios, R., Vanniere, B., Ziemen, F., Auger, L., et al. (2021). Tropical  
428 Cyclones in Global Storm-Resolving Models. *Journal of the Meteorological Society of*  
429 *Japan. Ser. II*, 99(3), 2021–029. <https://doi.org/10.2151/jmsj.2021-029>
- 430 Kaiser, M. J., & Yu, Y. (2010). The impact of Hurricanes Gustav and Ike on offshore oil and gas  
431 production in the Gulf of Mexico. *Applied Energy*, 87(1), 284–297.  
432 <https://doi.org/10.1016/j.apenergy.2009.07.014>
- 433 Kalnay, E., Kanamitsu, M., Kistler, R., Collins, W., Deaven, D., Gandin, L., et al. (1996). The  
434 NCEP/NCAR 40-year Reanalysis Project. *Bulletin of the American Meteorological Society*,  
435 (March).
- 436 Knutson, T., Camargo, S. J., Chan, J. C. L., Emanuel, K., Ho, C.-H., Kossin, J., et al. (2020).  
437 Tropical Cyclones and Climate Change Assessment: Part II: Projected Response to  
438 Anthropogenic Warming. *Bulletin of the American Meteorological Society*, 101(3), E303–  
439 E322. <https://doi.org/10.1175/BAMS-D-18-0194.1>
- 440 Landsea, C. W., & Franklin, J. L. (2013). Atlantic Hurricane Database Uncertainty and  
441 Presentation of a New Database Format. *Monthly Weather Review*, 141(10), 3576–3592.  
442 <https://doi.org/10.1175/MWR-D-12-00254.1>
- 443 Mangiavacchi, A., Rodenbusch, G., Radford, A., & Wisch, D. (2005). API Offshore Structure  
444 Standards: RP 2A and Much More. In *Offshore Technology Conference* (Vol. 2005-May,  
445 pp. 2195–2200). Offshore Technology Conference. <https://doi.org/10.4043/17697-MS>
- 446 Marks, D. G. (1992). *The beta and advection model for hurricane track forecasting*.
- 447 Mori, N., Yasuda, T., Mase, H., Tom, T., & Oku, Y. (2010). Projection of extreme wave climate  
448 change under global warming. *Hydrological Research Letters*, 4, 15–19.  
449 <https://doi.org/10.3178/HRL.4.15>

- Morim, J., Hemer, M., Wang, X. L., Cartwright, N., Trenham, C., Semedo, A., et al. (2019). Robustness and uncertainties in global multivariate wind-wave climate projections. *Nature Climate Change*, 9(9), 711–718. <https://doi.org/10.1038/s41558-019-0542-5>
- Moss, R. H., Edmonds, J. A., Hibbard, K. A., Manning, M. R., Rose, S. K., van Vuuren, D. P., et al. (2010). The next generation of scenarios for climate change research and assessment. *Nature*, 463(7282), 747–756.
- Oceanweather Inc. (2015). *GOMOS2014: Gulf of Mexico Oceanographic Study 2014. Project Description*. Stamford, CT, USA.
- Ojeda, E., Appendini, C. M., & Mendoza, E. T. (2017). Storm-wave trends in Mexican waters of the Gulf of Mexico and Caribbean Sea. *Natural Hazards and Earth System Sciences*, 17(8). <https://doi.org/10.5194/nhess-17-1305-2017>
- Panchang, V., Jeong, C. K., & Demirbilek, Z. (2013). Analyses of Extreme Wave Heights in the Gulf of Mexico for Offshore Engineering Applications. *Journal of Offshore Mechanics and Arctic Engineering*, 135(3), 31104–31115. <https://doi.org/10.1115/1.4023205>
- Roberts, M. J., Camp, J., Seddon, J., Vidale, P. L., Hodges, K., Vanniere, B., et al. (2020a). Impact of Model Resolution on Tropical Cyclone Simulation Using the HighResMIP–PRIMAVERA Multimodel Ensemble. *Journal of Climate*, 33(7), 2557–2583. <https://doi.org/10.1175/JCLI-D-19-0639.1>
- Roberts, M. J., Camp, J., Seddon, J., Vidale, P. L., Hodges, K., Vannière, B., et al. (2020b). Projected Future Changes in Tropical Cyclones Using the CMIP6 HighResMIP Multimodel Ensemble. *Geophysical Research Letters*, 47(14). <https://doi.org/10.1029/2020GL088662>
- Sørensen, O. R., Kofoed-Hansen, H., Rugbjerg, M., & Sørensen, L. S. (2004). A third-generation spectral wave model using an unstructured finite volume technique. In *Proceedings of the 29th International Conference on Coastal Engineering* (Vol. 2005-Janua, pp. 894–906). ASCE, New York. <https://doi.org/10.1142/9789812701916-0071>
- Timmermans, B., Stone, D., Wehner, M., & Krishnan, H. (2017). Impact of tropical cyclones on modeled extreme wind-wave climate. *Geophysical Research Letters*, 44(3), 1393–1401. <https://doi.org/10.1002/2016GL071681>
- Tolman, H. L. (2002). Alleviating the garden sprinkler effect in wind wave models. *Ocean*

*Modelling*, 4, 269–289.

Wisch, D. J., Puskar, F. J., Laurendine, T. T., O'Connor, P. E., Versowsky, P. E., &  
Bucknell, J. (2004). An Update on API RP 2A Section 17 for the Assessment of Existing  
Platforms. In *Offshore Technology Conference* (Vol. 3, pp. 2079–2089). OTC.  
<https://doi.org/10.4043/16820-MS>